Comparison of Torsional Vibration Controls based on the Fast and Slow Disturbance Observers

Yoichi Hori

Department of Electrical Engineering, University of Tokyo,
7-3-1 Hongo, Bunkyo, Tokyo 113, JAPAN
Fax: +81(3)5684-3986, E-mail: hori@kaya.t.u-tokyo.ac.jp

Abstract: *In recent steel rolling mill system, according to the application of high response AC drive system, the long shaft between the motor and the roll can no longer be assumed to be stiff. Vibration suppression and disturbance rejection are today's most important issue, and various control strategies have been proposed. In this paper, two relatively simple control techniques using the disturbance observer are proposed, analyzed and compared. One is the "resonance ratio control" based on the "fast disturbance observer". Another is the "slow disturbance observer". In both cases, by realizing "Manabe's Polynomial", the 2-mass non-stiff system can be controlled effectively, although there is a clear difference between these two techniques.*

INTRODUCTION

Vibration suppression and disturbance rejection in flexible system must be an important issue in the future motion control. It originates in the steel rolling mill system, where the load is coupled to the driving motor by a long shaft. As the newly required speed response is very close to the first resonant frequency of such systems, only the conventional techniques based on P&I control are not effective enough. To overcome the problems, various control strategies have been proposed mainly for controlling the 2-mass system, the simplest model of the flexible system.[4][5] Here, we can see the history of control theory: simple acceleration feedback, model following control, observer and state feedback, and modern H∞ control.

In this paper, I will propose and compare two relatively simple control techniques which uses the disturbance observer. One is the "resonance ratio control" based on the "fast disturbance observer". Another is the application of "slow disturbance observer". In both cases, by realizing "Manabe's Polynomial", the 2-mass system connected by a flexible shaft, the simplest model of flexible system, can be controlled effectively, although there is a clear difference between these two techniques.

First, the idea of "resonance ratio control" is explained. Resonance ratio is the ratio of the resonance and anti-resonance frequencies in 2-mass system. By using the torsional torque estimated by the "fast disturbance observer", the virtual motor inertia moment can be changed to any arbitrarily value. This means that we can change the resonance frequency and the virtual inertia ratio of the motor to the load. Yuki suggested that vibration can be suppressed effectively by adjusting the resonance ratio to be about $\sqrt{5}$.[6] I will show, in this paper, that $0.8\sqrt{5}$ is the optimal ratio in the speed control of the 2-mass system by realizing Manabe's model polynomial for P&I speed regulator.

The disturbance observer applied to the motor side has three design parameters, i.e., the cut-off frequency ω_o, the compensation gain *1-K* and the nominal inertia moment ratio *r*. ω_o of the "fast disturbance observer" is high enough so that its dynamics can be neglected. Instead, the gain *1-K* is not unity so as to be used for "resonance ratio control". In contrast, ω_o of the "slow disturbance observer" and *r* are the design parameters while the compensation gain is unity. "Slow disturbance observer" was originally proposed by Umida.[8] In this paper, I will show the optimal cut-off frequency and other controller parameters by realizing Manabe's polynomial.

SYSTEM MODEL

Figs.1 and 2 illustrate the typical steel rolling mill system configuration and its simplest model using two masses connected by a spring. Fig.3 shows the block diagram of the 2-mass system. Here I put

$$J_{M0} + J_L = 1\ ,\ K_s = 1 \qquad (1), (2)$$

These equations mean that the total inertia moment of the motor and the load, and the spring coefficient are fixed. Various 2-mass systems with different inertia ratios will be considered under these relations.

Fig.3 is the block diagram of the 2-mass system and Fig.4 illustrates the transfer function block diagram neglecting the disturbance T_L. Fig.4 is based on the coprime factorizations.

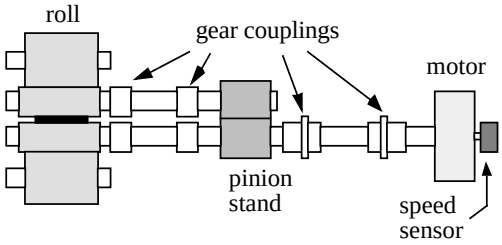

Fig.1 Illustration of the Steel Rolling Mill System.

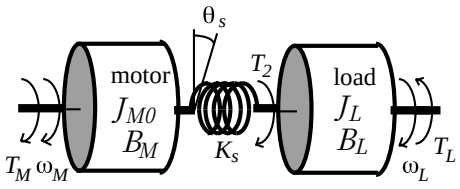

Fig.2 2-Mass System Model.

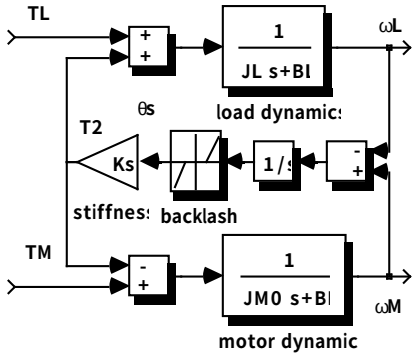

Fig.3 Block Diagram of the 2-Mass System.

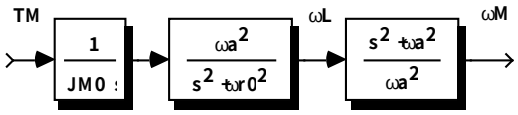

Fig.4 Transfer Function Representation.

An example of the frequency characteristics from T_M to ω_M is drawn in Fig.5. The resonant and anti-resonant frequencies are given by

$$\omega_{r0} = \sqrt{K_s\left(\frac{1}{J_{M0}} + \frac{1}{J_L}\right)} \tag{3}$$

and

$$\omega_a = \sqrt{\frac{K_s}{J_L}} \tag{4}$$

At these frequencies, the phase characteristic changes drastically.

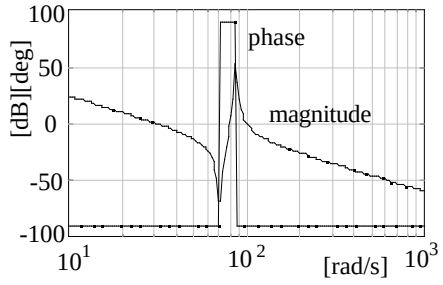

Fig.5 Frequency characteristics from ω_M to T_M.

The resonance ratio of the original system is defined by eq.(5).

$$H_0 = \frac{\omega_{r0}}{\omega_a} = \sqrt{1+\frac{J_L}{J_{M0}}} = \sqrt{1+R_0} \tag{5}$$

where R_0 is called the inertia ratio given by $R_0 = J_L/J_{M0}$.

RESONANCE RATIO CONTROL by FAST DISTURBANCE OBSERVER

Resonance Ratio Control

Fig.6 depicts how to perform the resonance ratio control using the disturbance observer. In usual disturbance rejection control systems, 100% of the estimated disturbance is fed back to the motor torque. In contrast, 1-K of the estimated disturbance is fed back in this case. One more block K is added in the path from the new control input T_M'.

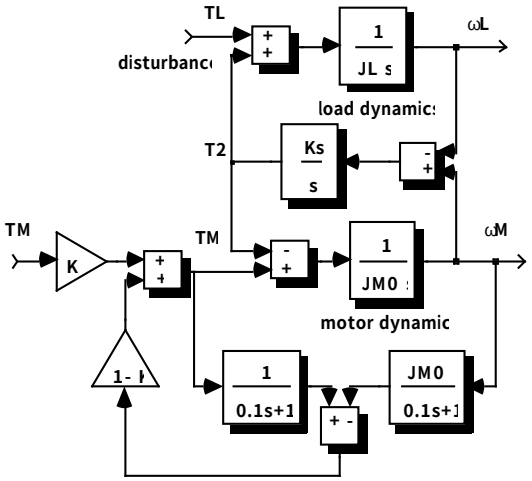

Fig.6 Block Diagram of the Resonance Control based on the Fast Disturbance Observer.

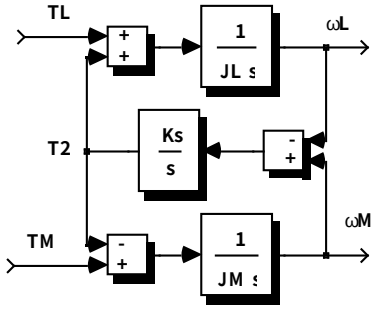

Fig.7 The Effect of the Resonance Ratio Control.

Fig.7 shows the new system where the resonance ratio control is applied. We can change the virtual motor inertia moment to any arbitrary value as given by

$$J_M = J_{M0}/K \tag{6}$$

This means that we can change the resonant frequency to

$$\omega_r = \sqrt{K_s\left(\frac{1}{J_M} + \frac{1}{J_L}\right)} \tag{7}$$

and the resonance ratio to

$$H = \sqrt{1+R} = \sqrt{1+\frac{J_L}{J_M}}$$

$$= \sqrt{1 + \frac{J_L}{J_{M0}/K}} = \sqrt{1 + R_0 K} \qquad (8)$$

From eq.(8), K to realize the optimal resonance ratio H can be obtained as given by

$$K = \frac{H^2 - 1}{R_0} \qquad (9)$$

Normalization

Fig.8 is the block diagram from the new input torque T_M' to the motor speed ω_M.

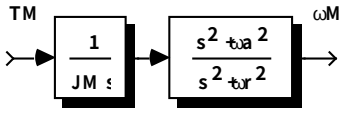

Fig.8 Block diagram from T_M' to ω_M.

For simplicity, the normalization using ω_a(=1) and J_L(=1) is introduced. The result is shown in Fig.9.

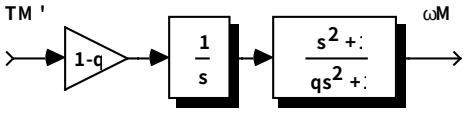

Fig.9 Normalized System by Putting ω_a=1 and J_L=1.

Relations among some variables are summarized as follows.

$$\omega_r = \sqrt{1+R}\,\omega_a = H\omega_a \qquad (10)$$
$$H = \sqrt{1+R} = 1/\sqrt{q} \qquad (11)$$
$$q = \frac{1}{H^2} = \frac{1}{1+R} < 1 \qquad (12)$$
$$\frac{J_L}{J_M} = R = H^2 - 1 = \frac{1}{q} - 1 \qquad (13)$$
$$\frac{J_M}{J_L} = \frac{1}{R} = \frac{1}{H^2 - 1} = \frac{q}{1-q} \qquad (14)$$

Controller Design using Manabe's Polynomial

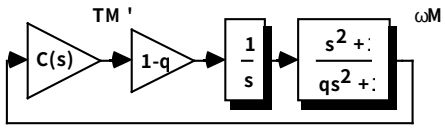

Fig.10 Design of Speed Controller *C(s)*.

Using P&I controller *C(s)*, the speed controller can be designed considering the closed loop characteristics (See Fig.10). When $C(s) = K_p + K_I/s$, the characteristic equation of the closed loop is given by

$$\begin{aligned} P(s) &= s^2(1+qs^2) + (K_p s + K_I)(1-q)(1+s^2) \\ &= qs^4 + K_p(1-q)s^3 + \{1+K_I(1-q)\}s^2 \\ &\qquad + K_p(1-q)s + K_I(1-q) \\ &= a_4 s^4 + a_3 s^3 + a_2 s^2 + a_1 s + a_0 \end{aligned} \qquad (15)$$

The relationship of Manabe's Polynomial[1][2][3] is given by

$$\tau = \frac{a_1}{a_0} = \frac{K_p(1-q)}{K_I(1-q)} = \frac{K_p}{K_I} \qquad (16)$$
$$\gamma_1 = \frac{a_1^2}{a_0\, a_2} = \frac{\{K_p(1-q)\}^2}{\{1+K_I(1-q)\}\, K_I(1-q)} = 2.5 \qquad (17)$$
$$\gamma_2 = \frac{a_2^2}{a_1\, a_3} = \frac{\{1+K_I(1-q)\}^2}{\{K_p(1-q)\}^2} = 2 \qquad (18)$$
$$\gamma_3 = \frac{a_3^2}{a_2\, a_4} = \frac{\{K_p(1-q)\}^2}{q\{1+K_I(1-q)\}} = 2 \qquad (19)$$

By solving these equations, we obtain

$$q = \frac{5}{16},\ H = \frac{4}{5}\sqrt{5},\ R = \frac{11}{5},\ J_M{:}J_L = 5{:}11 \qquad (20)$$

Eq.(20) means that $0.8\sqrt{5}$ is the optimal resonance ratio in this case.[7] Also, other normalized controller constants are uniquely calculated as

$$\tau = \frac{5\sqrt{2}}{2},\ K_p = \frac{10\sqrt{2}}{11},\ K_I = \frac{4}{11} \qquad (21),(22),(23)$$

The actual controller constants are given by

$$\tau = \frac{5\sqrt{2}}{2}\frac{1}{\omega_a},\ K_p = \frac{10\sqrt{2}}{11} J_L\omega_a \qquad (24),(25)$$
$$K_I = \frac{4}{11} J_L\omega_a^2 \qquad (26)$$

SLOW DISTURBANCE OBSERVER

Slow Disturbance Observer

Fig.11 shows the "slow disturbance observer" application. The disturbance observer applied to the motor side has three design parameters, i.e., the cut-off frequency ω_o , the compensation gain and the nominal inertia moment ratio *r*. The inertia moment used in the observer is $r\, J_{M0}$.

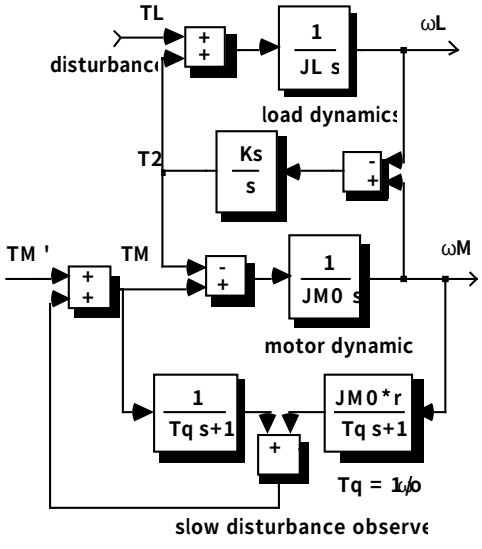

Fig.11 Application of the Slow Disturbance Observer

In the "fast disturbance observer" shown in Fig.6, its cut-off frequency was high enough so that the observer's dynamics can be neglected. In contrast to this, the cut-off frequency ω_o and the inertia moment ratio r are the design parameters in the "slow disturbance observer" while its compensation gain is 1.

The "slow disturbance observer" was originally proposed by Umida[8] and was improved by Iwata.[9] Umida proposed that the optimal cut-off frequency should be a little lower than the anti-resonant frequency ω_a. Iwata gave it as the simple function of ω_a and R_0, the inertia ratio. Here, I will try to derive the optimal cut-off frequency and the other parameters simultaneously by applying Manabe's polynomial.

Normalization

In this case, as we can not change the motor-side inertia moment, the normalization base is only ω_a. By putting ω_a=1, the 2-mass system given by Fig.4 is normalized as Fig.12.

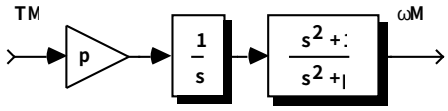

Fig.12 Normalized System by Putting ω_a=1.

Here, I put

$$p = H_0^2 = 1+R_0 = \frac{1}{J_M} \tag{27}$$

By applying the slow disturbance observer, the transfer function from T_M', the new controlled torque input, to ω_M is given by

$$\frac{\omega_M}{T_M'} = \frac{p}{s}\,\frac{(s+\omega_o)(s^2+1)}{s\,(s^2+p)+r\,\omega_o(s^2+1)} \tag{28}$$

Note that I use here the parameter r, the ratio of the inertia moment used in the disturbance observer to the actual motor inertia J_{M0}.

Controller Design using Manabe's Polynomial

Putting the P&I speed controller $C(s)$ as

$$K_p + \frac{K_I}{s} = K_p\,\frac{s+\omega_c}{s} \tag{29}$$

the characteristic equation of the closed loop system is given by

$$\begin{aligned} P(s) &= s^5 + (K_p p + r\,\omega_o)s^4 + \{K_p p(\omega_o+\omega_c)+p\}s^3 \\ &\quad + \{K_p p(\omega_o\omega_c+1)+r\,\omega\}s^2 + K_p p(\omega_o+\omega_c)s \\ &\quad + K_p p\omega_o\omega_c \\ &= a_5 s^5 + a_4 s^4 + a_3 s^3 + a_2 s^2 + a_1 s + a_0 \end{aligned} \tag{30}$$

The relationship of Manabe's Polynomial is given by the following equations.

$$\tau = \frac{a_1}{a_0} = \frac{\omega_o+\omega_c}{\omega_o\omega_c} \tag{31}$$

$$\gamma_1 = \frac{a_1^2}{a_0\,a_2} = \frac{\{K_p p(\omega_o+\omega_c)\}^2}{\{K_p p\omega_o\omega_c\}\{K_p p(\omega_o\omega_c+1)+r\,\omega\}} = 2.5 \tag{32}$$

$$\gamma_2 = \frac{a_2^2}{a_1\,a_3} = \frac{\{K_p p(\omega_o\omega_c+1)+r\,\omega\}^2}{\{K_p p(\omega_o+\omega_c)\}\{K_p p(\omega_o+\omega_c)+p\}} = 2 \tag{33}$$

$$\gamma_3 = \frac{a_3^2}{a_2\,a_4} = \frac{\{K_p p(\omega_o+\omega_c)+p\}^2}{\{K_p p(\omega_o\omega_c+1)+r\,\omega_o\}\{K_p p+r\,\omega_o\}} = 2 \tag{34}$$

$$\gamma_4 = \frac{a_4^2}{a_3\,a_5} = \frac{\{K_p p+r\,\omega_o\}^2}{\{K_p p(\omega_o+\omega_c)+p\}} = 2 \tag{35}$$

We should find four parameters ω_o, ω_c, K_p and r which satisfy the design condition given by eqs.(32)-(35).

The procedure to solve these equations are not very easy but the results are relatively simple. First, the equivalent time constant τ is given as a constant:

$$\tau = \sqrt{25+10\sqrt{5}} \approx 6.882 \tag{36}$$

I should omit the details, but one of the interesting results is that γ_4 is proportional to p, if other design conditions of eqs.(32)-(34) are satisfied. Regardless of the choice of r, γ_4 is given by

$$\gamma_4 = \frac{A^2}{B\,(\tau+B)}\,p \approx 0.6973\,p \tag{37}$$

A and B are given by eqs.(40) and (41) below.

When p increases, γ_4 becomes bigger. This means that the robustness is increased. However, for systems with smaller p, γ_4 is smaller and the system becomes easily unstable. To satisfy eq.(35): γ_4=2 exactly, $p=2B(\tau+B)/A^2$~2.8 should hold. This means R_0=1.8, which is very close to the easiest case also in the fast disturbance observer application.

Anyhow we can choose r as we like. Here I put $r = p$. This choice means that the disturbance observer uses the summation of motor and load inertia moments as the nominal inertia moment because

$$r\,J_{M0} = p\,J_{M0} = (1+R_0)J_{M0} = J_{M0}+J_L \tag{38}$$

By choosing r as this, other design parameters become constants regardless of p.

I should omit the detailed derivation but the observer's cut-off frequency ω_o is finally given as the real root of the following 3rd order equation (39).

$$B\,\omega_o^3 - A\,\omega_o^2 + \tau\,\omega_o - 1 = 0 \tag{39}$$

where

$$A = \frac{-1+\sqrt{681+304\sqrt{5}}}{2} \approx 17.944 \tag{40}$$

$$B = \sqrt{2A\,(1+A)} - \tau \approx 19.193 \tag{41}$$

By solving eq.(39), ω_o=0.3249is obtained. Accordingly P&I controller's parameters K_p and ω_c are given by

$$K_p = \frac{A}{B} - \omega_o \approx 0.6100 \qquad (42)$$

and

$$\omega_c = \frac{1}{B\,K_p\omega_o} \approx 0.2629 \qquad (43)$$

By multiplying ω_a, the actual ω_o and ω_c are obtained. As ω_a is the function of p (actually, $\omega_a=(\,p/(p-1)\,)^{1/2}$), ω_o and ω_c varies according to p.

SIMULATION RESULTS

Simulation results are shown for four different cases where the original systems' inertia ratios are 0.2, 1, 2 and 5. Fig.13 illustrates the simulation block diagram drawn by SIMULINK in Macintosh. Simulation is performed with 10~20% model errors, backlash (+/-0.01) and torque limiter (+/-1.2).

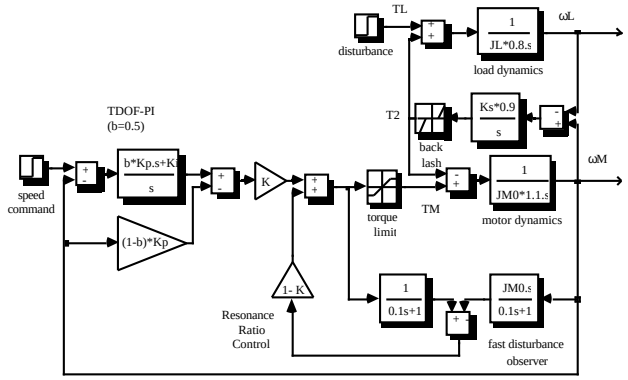

(a) Fast disturbance observer (resonance ratio control)

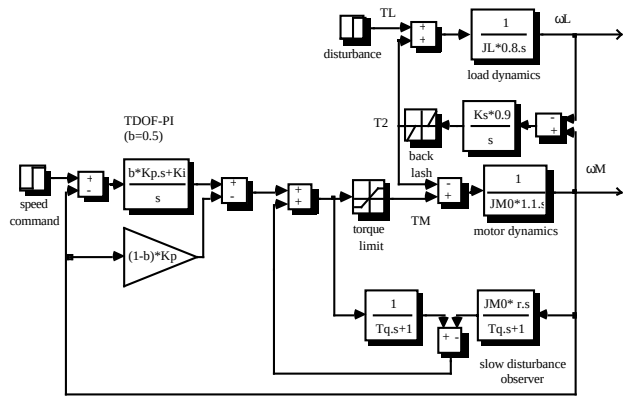

(b) Slow disturbance observer

Fig.13 Simulation block diagram with model error, backlash and torque limit.

Fig.14 shows the results of the resonance ratio control using the fast disturbance observer. From the various frequency characteristics plots, we can see the principle of the resonance control. In the time response simulation using SIMULINK, we can observe excellent performances both in the vibration suppression and the disturbance rejection. Moreover this method is quite effective to wide range of inertia ratio. We can see a slight performance degradation in Fig.14(a) where the inertia ratio is extremely small.

In Fig.14(a), we can also observe that the motor torque is negative for a while just after the disturbance torque is added at t=25. This means that the disturbance rejection and the vibration suppression are not consistent requirements for 2-mass systems with the inertia ratio R_0 smaller than 11/5=2.2.

In Fig.15, we can see the control performances of the "slow disturbance observer". In this type, we can not see any change of the resonant frequency but big damping effect around the resonant frequency is observed. The bigger the inertia ratio, the more robust to the parameter variation and backlash because γ_4 is big enough. In systems with smaller inertia ratio, robustness is weaker. This is because γ_4 becomes smaller when p is smaller as is given by eq.(37). However, too big γ_4 may mean an over-specification.

CONCLUSION

I proposed and compared two simple but effective control techniques for 2-mass system based on the disturbance observer. One is the "fast disturbance observer" to realize "resonance ratio control", and another is the "slow disturbance observer". In both cases, I tried to realize "Manabe's Polynomial" for their characteristic equations of the closed loop system. Although the obtained controllers are of only 2nd order system, their control performance is excellent. In particular, the fast disturbance observer is superior in operation through a wide range of the inertia ratio.

REFERENCES

[1] Graham, D. and Lathrop, R.C., The Synthesis of Optimum Transient Response: Criteria and Standard Forms, *AIEE Trans.*, Vol.72, pt.2, pp.273-288, 1953.

[2] Kessler, V.C., Ein Beitrag zur Theorie mehrschleifiger Regelungen, *Regelungstechnik*, H.8, pp.261-266, 1960.

[3] Manabe, S., Generalization of Classical, Optimal and H∞ Control Methods, *Journal of SICE*, Vol.30, No.10, pp.941-946, 1991.

[4] Hori, Y., Comparison of Vibration Suppression Control Strategies in 2-Mass Systems including a Novel Two-Degrees-Of-Freedom H∞ Controller, *IEEE 2nd AMC Workshop*, pp.409-416, 1992.

[5] Matsui, N. and Hori, Y., New Technologies on Motor Control, *Trans. of IEE-Japan*, Vol.113-D, No.10, pp.1122-1137, 1992.

[6] Yuki, K., Murakami, T. and Ohnishi, K., Vibration Control of a 2 Mass system by the Resonance Ratio Control, *Trans. of IEE-Japan*, Vol.113-D, No.10, 1993.

[7] Hori, Y., 2-Mass System Control based on Resonance Ratio Control and Manabe Polynomials, *Proc. of ASCC (First Asian Control Conference)*, Vol.3, pp.III-741-744, 1994.

[8] Umida, H., Novel Control Strategies of Torsional Vibration System: A Dully Tuned Disturbance Observer, *IEE-JapanIAS Annual Meeting*, S.12-3, 1994.

[9] Iwata, M., System Identification and Adaptive Vibration Control of a 2 Mass Resonant System, *IEE-Japan IAS Annual Meeting*, S.12-9, 1994.